Flare phenomenon in O-(2-[^{18}F]-Fluoroethyl)-L-Tyrosine PET after resection of gliomas

Christian P. Filss [1,2] , Ann K. Schmitz[3], Gabriele Stoffels[1], Carina Stegmayr[1], Philipp Lohmann[1], Jan Michael Werner[4], Michael Sabel[3,5], Marion Rapp[3], Roland Goldbrunner[5,6], Bernd Neumaier[1], Felix M. Mottaghy[2,5,7], N. Jon Shah[1,8], Gereon R. Fink [1,4], Norbert Galldiks[1,4,5], Karl-Josef Langen[1,2,5]

1) Institute of Neuroscience and Medicine (INM-3, INM-4, INM-5), Forschungszentrum Jülich, Jülich, Germany
2) Department of Nuclear Medicine, RWTH Aachen University, Aachen, Germany
3) Department of Neurosurgery, University of Düsseldorf, Düsseldorf, Germany
4) Department of Neurology, University of Cologne, Cologne, Germany
5) Center of Integrated Oncology (CIO), Universities of Aachen, Bonn, Cologne, and Düsseldorf, Germany
6) Department of Neurosurgery, University of Cologne, Cologne, Germany
7) Department of Radiology and Nuclear Medicine, Maastricht University Medical Center (MUMC+), Maastricht, The Netherlands
8) Department of Neurology, RWTH Aachen University, Aachen, Germany

Keywords: brain tumor surgery, amino acid PET, FET, treatment-related changes, extent of resection

Address for correspondence:
Karl-Josef Langen, M.D.
Institute of Neuroscience and Medicine
Forschnungszentrum Jülich
D-52425 Jülich, Germany
Phone: 0049-2461-61-5900
E-Mail: k.j.langen@fz-juelich.de

ABSTRACT

Purpose: PET using O-(2-[^{18}F]Fluoroethyl)-L-tyrosine (^{18}F-FET) is useful to detect residual tumor tissue after glioma resection. Recent animal experiments detected reactive changes of ^{18}F-FET uptake at the rim of the resection cavity within the first two weeks after resection of gliomas. In the present study, we evaluated pre- and postoperative ^{18}F-FET PET scans of glioma patients with particular emphasis on the identification of reactive changes after surgery.

Methods: Forty-three patients with cerebral gliomas (9 low-grade, 34 high-grade; 9 primary tumors, 34 recurrent tumors) who had preoperative (time before surgery, median 23 d, range 6-44 d) and postoperative ^{18}F-FET-PET (time after surgery, median 14, range 5–28 d) were included. PET scans (20-40 min p.i.) were evaluated visually for complete or incomplete resection (CR, IR) and compared with MRI. Changes of ^{18}F-FET-uptake in residual tumor were evaluated by tumor-to-brain ratios (TBR_{max}) and in the vicinity of the resection cavity by maximum lesion-to-brain ratios (LBR_{max}).

Results: Visual analysis of ^{18}F-FET PET scans revealed CR in 16/43 patients and IR in the remaining patients. PET results were concordant with MRI in 69% of the patients. LBR_{max} of ^{18}F-FET uptake in the vicinity of the resection cavity was significantly higher compared with preoperative values (1.59 ± 0.36 versus 1.14 ± 0.17; n=43, $p<0.001$). In 11 patients (26%) a “flare phenomenon” was observed with a considerable increase of ^{18}F-FET uptake compared with preoperative values in either the residual tumor (n=5) or in areas remote from tumor in the preoperative PET scan (n=6) (2.92 ± 1.24 versus 1.62 ± 0.75; $p<0.001$). Further follow-up in five patients showed decreasing ^{18}F-FET uptake in the flare areas in four and progress in one case.

Conclusions: Our study confirms that ^{18}F-FET PET provides valuable information for assessing the success of glioma resection. Postoperative reactive changes at the rim of the resection cavity appear to be mild. However, in 23 % of the patients, a postoperative “flare phenomenon” was observed that warrants further investigation.

INTRODUCTION

Cerebral gliomas are very difficult to treat due to their infiltrative growth, and prognosis remains very poor despite intensive multimodal treatment strategies (*1*). Surgical resection is the proposed first-line therapy, and the extent of tumor resection correlates with the efficacy of adjuvant treatment and prolonged survival (*2*,*3*). The standard method used to assess the amount of residual tumor following surgery is contrast-enhanced MRI. This should be performed within 72 h after surgery since later it becomes challenging to differentiate contrast-enhancing tumor tissue from treatment-related changes (*4*). Contrast enhancement in early postoperative MRI is, however, not a reliable measure of the extent of the residual tumor as considerable parts of gliomas may extend beyond the area of contrast enhancement and are not reliably detected by conventional MRI (*5*,*6*).

The potential of amino acid PET to determine the extent of glioma resection has been addressed in several studies, and, compared to conventional MRI a diagnostic gain has been consistently reported (*7*-*11*). PET using L-[methyl-^{11}C]-methionine (^{11}C-MET) successfully detected residual tumor tissue in 13 out of 19 pediatric brain tumors, which were confirmed by repeated surgery or tumor progress in all cases (*7*). In another study including 43 adult patients with high-grade glioma, total tumor resection as assessed by ^{11}C-MET PET, correlated significantly with survival, while a total removal of contrast enhancement in MRI did not (*8*). For PET using O-(2-^{18}F-Fluoroethyl)-L-tyrosine (^{18}F-FET), the most extensive study to date (n=62) reported conflicting findings compared to MRI in 19% of patients after resection of gliomas (*11*). Furthermore, elevated tracer uptake on the postoperative ^{18}F-FET-PET scans correlated with the sites of subsequent tumor recurrence (*12*).

A recent study showed residual ^{18}F-FET uptake after surgery beyond intraoperative fluorescence after the application of 5-aminolevulinic acid in 13 of 31 patients with glioblastoma (*10*).

In a recent experimental study with rat gliomas, we observed increased ^{18}F-FET uptake at the rim of the resection cavity within the first two weeks following glioma resection, especially in the first few days after surgery (*13*). Since this uptake decreased in the second week after surgery, it was recommended that ^{18}F-FET PET should be performed later than two weeks after resection. In this retrospective study, we evaluated the pre- and postoperative ^{18}F-FET PET scans of glioma patients with particular emphasis on potential reactive changes after surgery.

MATERIAL AND METHODS

Patient Population

We searched our records of the last ten years for patients with cerebral gliomas who had undergone preoperative ^{18}F-FET PET and postoperative control within four weeks after surgery as part of clinical diagnostics. Forty-three patients met these criteria who had preoperative (time before surgery, median 23 d, range 6-44 d) and postoperative ^{18}F-FET-PET (time after surgery, median 14, range 5–28 d). Ten of the patients had untreated primary tumors, and 33 patients had tumor relapse after various forms of pre-treatment. A detailed overview of the histopathological diagnosis and clinical data of the patients is presented in Table 1. Histopathological diagnosis was based on the World Health Organization (WHO) classification of 2007 since no molecular markers were available for the older cases (*14*). A further subdivision of the patients was made concerning the time interval of ^{18}F-FET PET investigation after surgery (Fig.1), according to our previous study (*13*). Group A (n=23) had the second ^{18}F-FET PET within 5-14 days following tumor resection and group B was within 15-28 days (n=20). The resection status according to early postoperative MRI (< 48 h post-op) was available for 39 patients, and 15 patients had additional

^{18}F-FET PET scans in the further course of the disease (mean, 193 days; range, 54-389 days post-op).

^{18}F-FET PET

Dynamic PET data were acquired for 40 min after intravenous injection of approx. 2.5 MBq of ^{18}F-FET/kg of body weight. Seventy-nine scans were obtained using a stand-alone PET scanner (ECAT EXACT HR+, Siemens Healthcare, Erlangen, Germany) and 22 scans on a high-resolution 3T hybrid PET/MR scanner (BrainPET, Siemens Healthcare). Further details are given in the supplemental material.

PET Data Analysis

^{18}F-FET uptake in the tissue was expressed as standardized uptake value (SUV) by dividing the radioactivity concentration (kBq/ml) in the tissue by the radioactivity injected per gram of body weight. The summed ^{18}F-FET PET images (20 to 40 min p.i.) were used for further analysis. The different ^{18}F-FET PET and MRI scans of the individual patients were coregistered using the commercially available software PMOD, version 3.408. In a first step, the pre- and postoperative PET images were visually evaluated by two physicians experienced in ^{18}F-FET PET reading (K.-J.L., C.P.F.) and classified in consensus as i) complete resection, if no significant residual pathological ^{18}F-FET uptake was detectable after surgery, and ii) incomplete resection, if pathological ^{18}F-FET uptake was present after surgery. Furthermore, cases with a prominent increase of local or distant ^{18}F-FET accumulation in the post-surgical PET scans were evaluated separately.

For quantitative evaluation, spherical volumes of interest (VOI) with a volume of 2 ml were used, as this reduces the influence of different scanner resolutions (*15*). A crescent-shaped reference ROI, placed in the contralateral hemisphere in an area of normal-appearing brain tissue served as a background region. Maximum tumor-to-brain ratios (TBR_{max}) or maximum lesion-to-brain ratios (LBR_{max}) were calculated by dividing the SUV in those VOIs by the mean SUV in the background region (*16*). In order to evaluate reactive changes induced by surgery, 2 ml VOIs were placed in the postoperative PET scans at the rim of the resection cavity, which were free of tumor according to the pre- and postoperative PET and MRI scan. The LBR_{max} of these VOIs were compared to preoperative values.

In cases with a prominent increase of local or distant ^{18}F-FET accumulation in PET scans after surgery, 2 ml VOIs were centered on the maximum of these areas with presumable tumor tissue and the TBR_{max} was compared to preoperative values after the projection of these VOIs to the preoperative PET scans. Furthermore, the biological tumor volume (BTV) was determined using a threshold of 1.6 above the reference value. This has been described to best separate primary tumor from non-tumoral tissue in a biopsy controlled study (*17*). Pre- and postoperative BTV were compared. Furthermore, time-activity-curves (TAC) of ^{18}F-FET-uptake in those areas were evaluated and the time-to-peak (TTP) and the slope of the TAC in the late phase of ^{18}F-FET uptake was determined (see supplemental material).

Statistical Analysis

Descriptive statistics are provided as mean and standard deviation and/or median and range. The Student t-test for independent samples was used to compare two groups, and the paired t-test for dependent samples for the analysis of changes after therapy. The Mann-Whitney rank-sum test

was used when variables were not normally distributed. Categorical variables were tested by Pearson's chi-squared test or Fisher's exact test. Data analysis was carried out with SigmaPlot Version 11.0 (Systat Software, San José, CA, USA). Probability values of less than 0.05 were considered significant.

RESULTS

Visual analysis of ^{18}F-FET PET scans yielded CR in 16 patients and IR in 27 patients. PET results were concordant with early postoperative MRI in 69% of the patients, i.e., 13% had CR of contrast-enhancing tissue in MRI and 56% IR. In 31% of patients, the results of PET and MRI were discordant, i.e., 8% showed CR in MRI but IR in PET and 23% IR in MRI but CR in PET. ^{18}F-FET uptake in the vicinity of the resection cavity was significantly increased compared with preoperative values (LBR 1.59 ± 0.36 versus 1.14 ± 0.17; $p<0.001$). There was no significant difference in the changes of the LBR in the vicinity of the resection cavity in group A and group B. An example of increased ^{18}F-FET uptake in the vicinity of the resection cavity is presented in Figure 2.

The median BTV of ^{18}F-FET uptake before surgery was 18 ml (range 2 – 162 ml) and 22 ml after surgery (range 4-222 ml). The BTV decreased after surgery in 16 patients and increased in 27 patients. An increasing BTV after surgery occurred significantly more frequent in group A than in group B (18 vs. 9, $p = 0.03$). Importantly, nine patients of the patients with CR of ^{18}F-FET uptake according to visual evaluation (n =18) showed increasing values of BTV after surgery.

A prominent increase of regional ^{18}F-FET accumulation after surgery was observed in 11 patients (26 %) (TBR_{max} 2.92 ± 1.24 versus 1.62 ± 0.75; $p<0.001$) and will subsequently be referred to as “flare phenomenon”. The flare phenomenon occurred significantly more frequent in group 2 (n=9) than in group 1 (n=2; p=0.01). In five patients, the flare phenomenon occurred in the residual tumor after surgery, i.e., in the area that showed highly tumor suspicious ^{18}F-FET uptake in the preoperative scan. In six patients, the flare phenomenon occurred in areas remote from the area of increased tracer uptake in the preoperative PET scan. The relative changes of the TBR_{max} in these patients are shown in Figure 3. In five cases MRI showed contrast enhancement in the flare region

and in six cases not. T2-weighted MRI was abnormal in the flare region in all cases. Analysis of the TAC of ^{18}F-FET upake in the flare areas showed no significant change between pre-OP and post OP values (time-to-peak: 28.5 ± 8.1 min versus 27.5 ± 10.3 min; slope: 0.33 ± 0.58 versus 0.23 ± 0.94 SUV/h; n=11, n.s.). In six patients, the slope in the flare area showed an increase both pre OP and post OP, in three cases an increase pre OP and a decrease post OP and in 2 cases a decrease both pre OP and post OP. In four of the 11 cases with flare phenomenon, a follow-up ^{18}F-FET PET was available that showed a decreasing ^{18}F-FET uptake in the flare area during radiochemotherapy in three cases and further increasing ^{18}F-FET uptake with tumor progression in one case. Examples of flare phenomena in areas remote from the area of increased tracer uptake in the preoperative PET scan in residual tumor tissue are shown in Figures 4 and in supplemental Figure 1. In the latter case, the area with flare phenomenon exhibited tumor progression after three months.

DISCUSSION

As outlined in the introduction, the value of amino acid PET in the assessment of glioma resection has been investigated in several studies and it has been consistently demonstrated that its use in this diagnostic question provides important additional information in comparison to MRI. In contrast with previous studies, the present study provides compelling new aspects regarding surgery-induced changes in ^{18}F-FET accumulation and the occurrence of a flare phenomenon.

Concerning the visual assessment of the resection status, we observed an agreement between ^{18}F-FET PET and MRI in 69% of the patients in this study (13% CR, 56% IR), which is largely consistent with the results from Pirotte et al. (*8*) who reported an agreement between

postsurgical ^{11}C-MET PET and MRI in 67% of the patients (23% CR, 44% IR). The study by Buchmann et al. reported a higher agreement between ^{18}F-FET PET and MRI of 81% (44% CR, 37% IR) (*11*). In that study, the presence of residual tumor tissue in ^{18}F-FET PET was not based on visual analysis but rather on the quantitative evaluation of the BTV only, i.e., the presence of tissue with an ^{18}F-FET tumor-to-brain ratio of 1.6 or more compared with normal brain tissue. The authors reported no residual ^{18}F-FET uptake (BTV = 0 ml) after surgery in 49% of the patients, which is surprising since this was not observed in any case in the current study or in the study by Mühter et al.(*10*). This discrepancy may be explained by a different definition of the background ROI (*18*), but it certainly raises questions about the comparability of the different studies.

In a recent experimental study with rat gliomas, we observed treatment-related ^{18}F-FET uptake with a mean LBR of 2.0 ± 0.3 at the rim of the resection cavity, which is well above the limit of 1.6. In agreement with these animal experiments, in this study, we observed increased ^{18}F-FET uptake in the vicinity of the resection cavity after surgery, and a LBR > 1.6 was noted in all patients (smallest BTV = 4 ml). Our data suggest that reactive changes of ^{18}F-FET uptake after surgery are a common phenomenon (Fig. 2) and should be carefully considered when assessing residual tumor tissue. We suggest that the determination of BTV based on a ratio of > 1.6 compared with normal brain tissue is not a reliable method for determining residual tumor volume in the early postoperative situation.

Interestingly, an increasing BTV after surgery occurred more frequently in group 1 than in group 2 (18 vs. nine cases), suggesting that reactive changes of ^{18}F-FET uptake after surgery are more pronounced in the first two weeks after surgery than in weeks 3–4. This observation is in line with the animal experiments mentioned above, which demonstrated a decrease of reactive changes of ^{18}F-FET uptake 14 days after surgery.

A striking discovery of our study is the observation of a flare phenomenon of ^{18}F-FET uptake after surgery, which has not been reported in previous studies (*7,10,11*). This phenomenon was found in 26% of patients and cannot be considered as an exceptional observation. In five cases, flare was observed in the area of the preoperatively detectable tumor tissue and in six cases it was observed at distant sites which showed only a slightly increased ^{18}F-FET accumulation in the preoperative ^{18}F-FET PET (Fig. 4 and supplemental Figure 1). Moreover, it occurred significantly more frequently in patient group B than in patient group A. Further follow-up, which was available in four cases, showed a decreasing ^{18}F-FET uptake in the flare area during radiochemotherapy in three cases (Fig. 4) and further increasing ^{18}F-FET uptake corresponding with tumor progression in one case (Supplemental Fig. 1).

Several hypotheses may help to explain this phenomenon. Firstly, the flare phenomenon might be caused by reactive astrocytosis. This explanation appears unlikely, because in previous animal studies ^{18}F-FET uptake in areas of reactive astrocytosis around the resection cavity was only moderately increased and not as pronounced as in the flare areas, which often occurred in remote regions (*13*). Another explanation may be a rapid tumor progression, which is not unusual in glioblastoma, but as the flare phenomenon occurred also in two cases of oligodendroglioma, this explanation also seems implausible. Thus, a more likely hypothesis is the assumption that surgical intervention stimulated the metabolic activity of infiltrating tumor tissue with low metabolic activity before surgery. Accumulative evidence suggests that the tissue response to surgical brain injury participates in the formation of recurrence-prone microenvironments (*19,20*). Experiments in a murine glioma resection and recurrence model demonstrated that surgical injury to astrocytes promotes tumor proliferation and migration (*19,21*). It is tempting, therefore, to speculate that ^{18}F-FET PET could discover such kind of tumor activation after surgery.

The results of this study are limited by the fact that the observed changes in ^{18}F-FET PET after surgery were not histologically confirmed and not systematically evaluated by further follow-up. Furthermore, the majority of the patients had been treated previously and it may not be correct to extrapolate these findings to patients undergoing initial resection of glioma. Therefore, further investigation and confirmation of these results by prospective studies are necessary. Nevertheless, reactive changes in ^{18}F-FET PET at the rim of the resection cavities should be considered in postoperative scan readings since they are in line with experimental studies, and histological clarification of these changes is difficult to carry out for ethical reasons.

CONCLUSION

Our study confirms that ^{18}F-FET PET adds valuable information in the assessment of patients with glioma following resection. Postoperative reactive changes at the rim of the resection cavity have to be considered, especially in the first two weeks after surgery. In a considerable number of patients, a postoperative flare phenomenon was observed that needs further investigation.

Competing Interests

The authors declare that they have no competing interests.

Ethics Approval and Consent to Participate

All subjects gave prior written informed consent for their participation in the ^{18}F-FET PET study and evaluation of their data for scientific purposes. The local ethics committee approved the

evaluation of retrospectively collected patient data. All procedures performed in studies involving human participants followed the national ethical standards and the Declaration of Helsinki.

ACKNOWLEDGEMENTS

The authors thank Erika Wabbals, Silke Grafmueller, and Sascha Rehbein for technical assistance in radiosynthesis of ^{18}F-FET, and Silke Frensch, Suzanne Schaden, Natalie Judov, Kornelia Frey, and Trude Plum for technical assistance in performing the PET measurements.

KEY POINTS

Question: Does the resection of cerebral gliomas lead to increased ^{18}F-FET accumulation in reactive tissue?

Pertinent findings: In a retrospective study ^{18}F-FET uptake was analyzed before and after surgery in 43 patients with cerebral gliomas. A moderate but significant increase of ^{18}F-FET uptake was noted at the rim of resection cavity. Unexpectedly, a postoperative flare phenomenon was observed in 26 % of the patients, possibly reflecting activation of residual tumor tissue by surgical injury.

Implications for patient care: ^{18}F-FET PET is helpful in assessing glioma resection, but the intervention can also lead to increased tracer uptake, which must be considered when assessing the extent of glioma resection

REFERENCES

1. Weller M, van den Bent M, Tonn JC, et al. European Association for Neuro-Oncology (EANO) guideline on the diagnosis and treatment of adult astrocytic and oligodendroglial gliomas. *Lancet Oncol.* 2017;18:e315-e329.

2. Kuhnt D, Becker A, Ganslandt O, Bauer M, Buchfelder M, Nimsky C. Correlation of the extent of tumor volume resection and patient survival in surgery of glioblastoma multiforme with high-field intraoperative MRI guidance. *Neuro Oncol.* 2011;13:1339-1348.

3. Oszvald A, Guresir E, Setzer M, et al. Glioblastoma therapy in the elderly and the importance of the extent of resection regardless of age. *J Neurosurg.* 2012;116:357-364.

4. Forsting M, Albert FK, Kunze S, Adams HP, Zenner D, Sartor K. Extirpation of glioblastomas: MR and CT follow-up of residual tumor and regrowth patterns. *AJNR Am J Neuroradiol.* 1993;14:77-87.

5. Scott JN, Brasher PM, Sevick RJ, Rewcastle NB, Forsyth PA. How often are nonenhancing supratentorial gliomas malignant? A population study. *Neurology.* 2002;59:947-949.

6. Lohmann P, Stavrinou P, Lipke K, et al. FET PET reveals considerable spatial differences in tumour burden compared to conventional MRI in newly diagnosed glioblastoma. *Eur J Nucl Med Mol Imaging.* 2019;46:591-602.

7. Pirotte B, Levivier M, Morelli D, et al. Positron emission tomography for the early postsurgical evaluation of pediatric brain tumors. *Childs Nerv Syst.* 2005;21:294-300.

8. Pirotte BJ, Levivier M, Goldman S, et al. Positron emission tomography-guided volumetric resection of supratentorial high-grade gliomas: a survival analysis in 66 consecutive patients. *Neurosurgery.* 2009;64:471-481.

9. Pirotte BJ, Lubansu A, Massager N, et al. Clinical impact of integrating positron emission tomography during surgery in 85 children with brain tumors. *J Neurosurg Pediatr.* 2010;5:486-499.

10. Muther M, Koch R, Weckesser M, Sporns P, Schwindt W, Stummer W. 5-Aminolevulinic Acid Fluorescence-Guided Resection of 18F-FET-PET Positive Tumor Beyond Gadolinium Enhancing Tumor Improves Survival in Glioblastoma. *Neurosurgery.* 2019;85:E1020-E1029.

11. Buchmann N, Klasner B, Gempt J, et al. (18)F-fluoroethyl-l-tyrosine positron emission tomography to delineate tumor residuals after glioblastoma resection: a comparison with standard postoperative magnetic resonance imaging. *World Neurosurg.* 2016;89:420-426.

12. Buchmann N, Gempt J, Ryang YM, et al. Can Early Postoperative O-(2-(18F)Fluoroethyl)-l-Tyrosine Positron Emission Tomography After Resection of Glioblastoma Predict the Location of Later Tumor Recurrence? *World Neurosurg.* 2019;121:e467-e474.

13. Geisler S, Stegmayr C, Niemitz N, et al. Treatment-Related Uptake of O-(2-(18)F-Fluoroethyl)-l-Tyrosine and l-[Methyl-(3)H]-Methionine After Tumor Resection in Rat Glioma Models. *J Nucl Med.* 2019;60:1373-1379.

14. Louis DN, Ohgaki H, Wiestler OD, et al. The 2007 WHO classification of tumours of the central nervous system. *Acta Neuropathol.* 2007;114:97-109.

15. Filss CP, Albert NL, Boning G, et al. O-(2-[(18)F]fluoroethyl)-L-tyrosine PET in gliomas: influence of data processing in different centres. *EJNMMI Res.* 2017;7:64.

16. Law I, Albert NL, Arbizu J, et al. Joint EANM/EANO/RANO practice guidelines/SNMMI procedure standards for imaging of gliomas using PET with radiolabelled amino acids and [(18)F]FDG: version 1.0. *Eur J Nucl Med Mol Imaging.* 2019;46:540-557.

17. Pauleit D, Floeth F, Hamacher K, et al. O-(2-[18F]fluoroethyl)-L-tyrosine PET combined with MRI improves the diagnostic assessment of cerebral gliomas. *Brain.* 2005;128:678-687.

18. Unterrainer M, Vettermann F, Brendel M, et al. Towards standardization of 18F-FET PET imaging: do we need a consistent method of background activity assessment? *EJNMMI Res.* 2017;7:48.

19. Okolie O, Bago JR, Schmid RS, et al. Reactive astrocytes potentiate tumor aggressiveness in a murine glioma resection and recurrence model. *Neuro Oncol.* 2016;18:1622-1633.

20. Hamard L, Ratel D, Selek L, Berger F, van der Sanden B, Wion D. The brain tissue response to surgical injury and its possible contribution to glioma recurrence. *J Neurooncol.* 2016;128:1-8.

21. Ratel D, van der Sanden B, Wion D. Glioma resection and tumor recurrence: back to Semmelweis. *Neuro Oncol.* 2016;18:1688-1689.

Table 1

Patient Number	Sex	Age (years)	Histo	Prim/Rec	Pretreatment	MRI	FET PET	Interval between surgery and FET PET	LBR_{max} rim pre OP	LBR_{max} rim post OP	BTV pre OP	BTV post OP	Flare Phenomenon	TBR_{max} pre OP	TBR_{max} post OP
1	M	54	AII	Rec	S	IR	CR	5	1.1	1.4	1.5	3.9	**no**	-	-
2	F	39	AII	Rec	S/Ch	IR	IR	6	1.1	1.3	13.6	22.4	**no**	2.56	1.85-
3	F	50	GBM	Prim	no	CR	CR	6	1.5	2.1	21.2	30.4	**no**	-	-
4	M	27	AII	Prim	no	IR	IR	6	1.2	1.4	26.7	13.0	**no**	2.69	2.34
5	F	77	AIII	Rec	S	IR	CR	7	1.0	1.8	2.9	12.1	**no**	-	-
6	M	43	OIII	Rec	S/Ch	CR	CR	8	1.0	1.5	17.0	4.8	**no**	-	-
7	M	45	GBM	Rec	S/R/Ch	IR	CR	9	1.2	1.2	12.6	8.3	**no**	-	-
8	F	15	GBM	Prim	S	n.a.	IR	9	1.2	2.0	39.8	57.9	**no**	4.54	2.38-
9	M	57	AII	Prim	no	IR	IR	10	1.2	1.1	85.3	43.9	**no**	2.28	2.35
10	M	42	OAIII	Rec	S/R/Ch	IR	IR	12	0.8	1.7	21.8	34.6	**no**	3.33	2.07-
11	M	38	AIII	Rec	S/R/Ch	IR	IR	12	1.6	1.7	14.3	18.8	**no**	3.08	3.09
12	M	33	GBM	Rec	S/R/Ch	IR	CR	12	1.1	1.7	17.5	27.0	**no**	-	-
13	M	38	OII	Rec	S	CR	IR	12	1.0	1.3	6.9	6.2	**no**	2.49	1.74
14	F	26	OAII	Rec	S/Ch	IR	IR	12	1.2	2.0	162.6	220.5	**no**	6.12	6.69
15	M	35	OAIII	Rec	S/Ch	IR	IR	13	1.1	1.3	11.7	18.4	**no**	3.33	3.14
16	M	51	GBM	Rec	S/R/Ch	IR	CR	13	1.0	1.3	3.7	6.9	**no**	-	-
17	M	53	GBM	Prim	no	CR	IR	13	1.2	2.0	20.1	81.7	**distant**	1.26	3.37
18	M	39	GBM	Rec	S/R/Ch	IR	IR	13	1.1	1.6	4.0	24.3	**distant**	0.99	1.82
19	F	27	AIII	Rec	S/Ch	IR	IR	13	1.0	1.5	18.0	55.8	**no**	2.26	1.98
20	M	71	AIII	Rec	S/R/Ch	CR	IR	13	1.0	1.4	31.8	45.5	**no**	2.22	2.47
21	M	30	AII	Prim	no	IR	CR	13	1.2	1.6	2.9	15.8	**no**	-	-
22	M	29	AIII	Rec	S/Ch	IR	IR	14	1.2	1.6	26.0	40.3	**no**	2.00	2,10
23	M	63	OAII	Rec	S	IR	IR	14	1.1	1.5	7.3	16.0	**no**	2.25	1.82
24	M	49	GBM	Rec	S/R/Ch	IR	CR	15	1.0	1.4	11.5	8.8	**no**	-	-
25	M	51	OAIII	Rec	S/R/Ch	IR	IR	15	1.5	1.8	81.4	62.5	**local**	3.61	5.28
26	F	55	GBM	Rec	S/R/Ch	CR	CR	15	1.1	1.4	18.9	9.0	**no**	-	-
27	M	54	GBM	Rec	S/R/Ch	IR	IR	15	0.9	1.6	71.0	59.9	**no**	3.18	2.46
28	F	74	GBM	Rec	S/R/Ch	CR	CR	16	1.2	1.5	11.2	7.5	**no**	-	-
29	F	73	GBM	Prim	no	n.a.	CR	17	1.2	1.2	49.1	6.8	**no**	-	-
30	M	86	AII	Rec	S/R/Ch	n.a.	CR	17	1.0	1.3	8.8	6.0	**no**	-	-
31	F	53	GBM	Rec	S/R/Ch	IR	IR	18	1.1	1.8	13.0	33.0	**local**	1.45	1.97
32	F	45	OA II	Rec	S	IR	IR	18	1.1	1.4	50.9	39.8	**no**	2.63	2.34
33	F	38	OIII	Rec	S/Ch	IR	IR	18	0.9	1.9	19.0	30.9	**distant**	1.54	2.91
34	M	68	GBM	Prim	no	IR	IR	18	1.4	3.2	67.5	146.5	**distant**	1.99	5.01
35	M	66	GBM	Rec	S/R/Ch	n.a.	IR	19	0.9	1.2	28.3	42.5	**distant**	1.74	2.81
36	M	37	OII	Rec	S/Ch	IR	IR	20	1.3	2.0	25.3	35.0	**local**	1.15	2.08
37	F	63	AIII	Prim	no	IR	IR	21	1.0	1.4	6.9	17.4	**local**	1.38	2.49
38	M	72	AIII	Rec	S/R/Ch	IR	IR	21	0.9	1.8	96.5	153.5	**local**	1.84	2.93
39	F	79	GBM	Rec	S/R/Ch	IR	IR	21	1.2	1.4	2.6	4.2	**distant**	0.86	1.46
40	F	62	GBM	Prim	S/R/Ch	IR	CR	26	1.0	1.3	13.3	9.9	**no**	-	-
41	M	55	OAIII	Rec	S/R/Ch	IR	CR	27	1.0	1.5	8.1	16.0	**no**	-	-
42	M	51	GBM	Rec	S/R/Ch	CR	CR	28	1.5	1.7	85.9	45.2	**no**	-	-
43	F	57	AIII	Prim	no	IR	IR	28	1.1	1.6	14.4	10.0	**no**	2.40	2.39

M = male; **F** = female; **GBM =** glioblastoma; **A** = astrocytoma; **O** = oligodendroglioma; **OA** = oligoastrocytoma; **I - III** = tumor grade according to WHO classification 2007; **Prim** = untreated primary tumor; **Rec** = recurrent tumor; **S** = surgery; **R** = radiotherapy; **Ch** = chemotherapy; **LBR rim** = lesion-to-brain ratio of ^{18}F-FET uptake at the rim of the resection cavity; **TBR_{max}** = maximum tumor-to-brain ratio; **BTV** = biological tumor volume with a TBR > 1.6; **Local /distant flare phenomenon:** prominent increase of ^{18}F-FET uptake after surgery in the area of tumor tissue with increased ^{18}F-FET uptake in the preoperative scan (local) or in an area distant to that location

Figures

Figure 1:

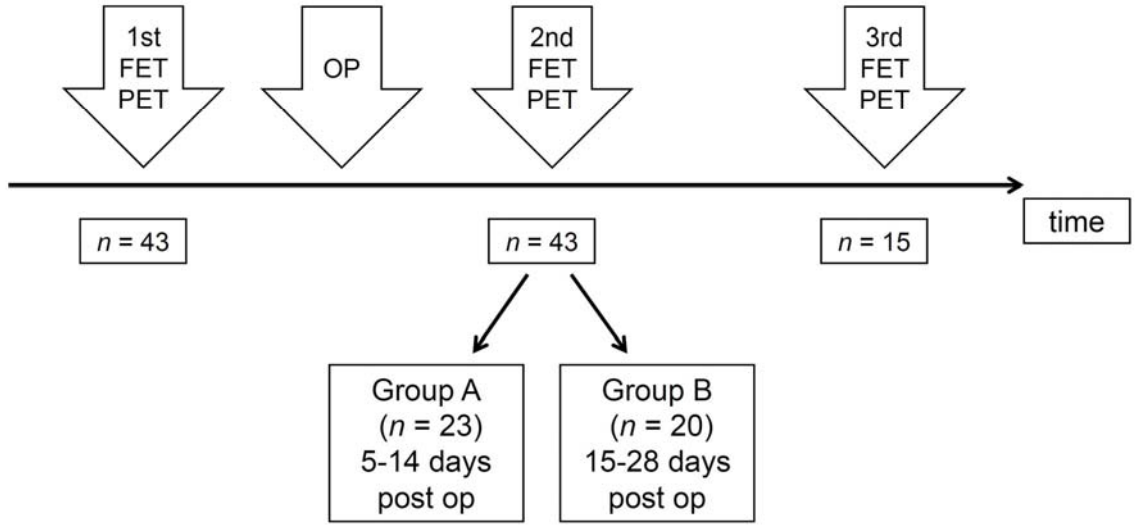

Schematic time course of ^{18}F-FET PET

Figure 2

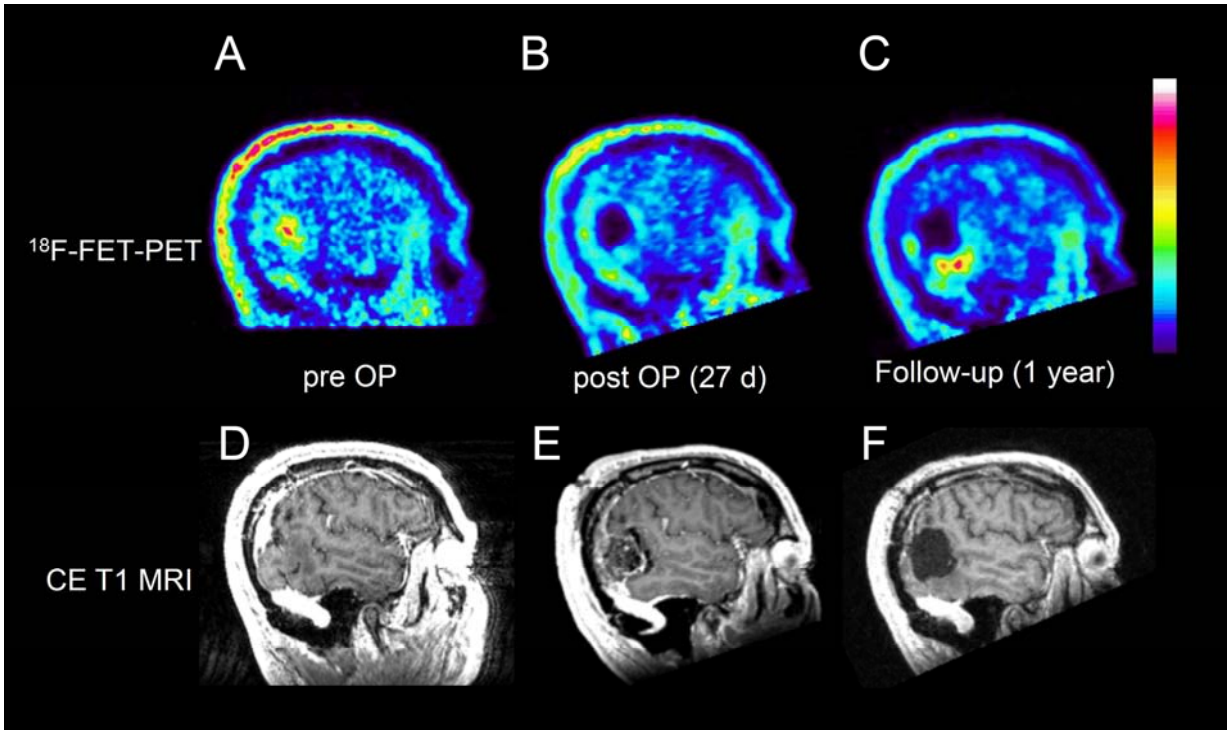

Patient with a recurrent oligoastrocytoma WHO grade III (Pat. No 41). Sagittal slices of pre-, postoperative, and follow-up ^{18}F-FET PET (A - C), and contrast-enhanced T1-weighted MRI (D - F). Postoperative ^{18}F-FET PET (B) is rated as CR of the tumor, but there is slightly increased tracer uptake at the rim of the resection cavity (LBR_{max} 1.5) interpreted as reactive changes. The measured BTV increases from 8 to 16 ml after surgery. Follow-up after one year shows recurrent tumor at the lower rim of the resection cavity.

Figure 3

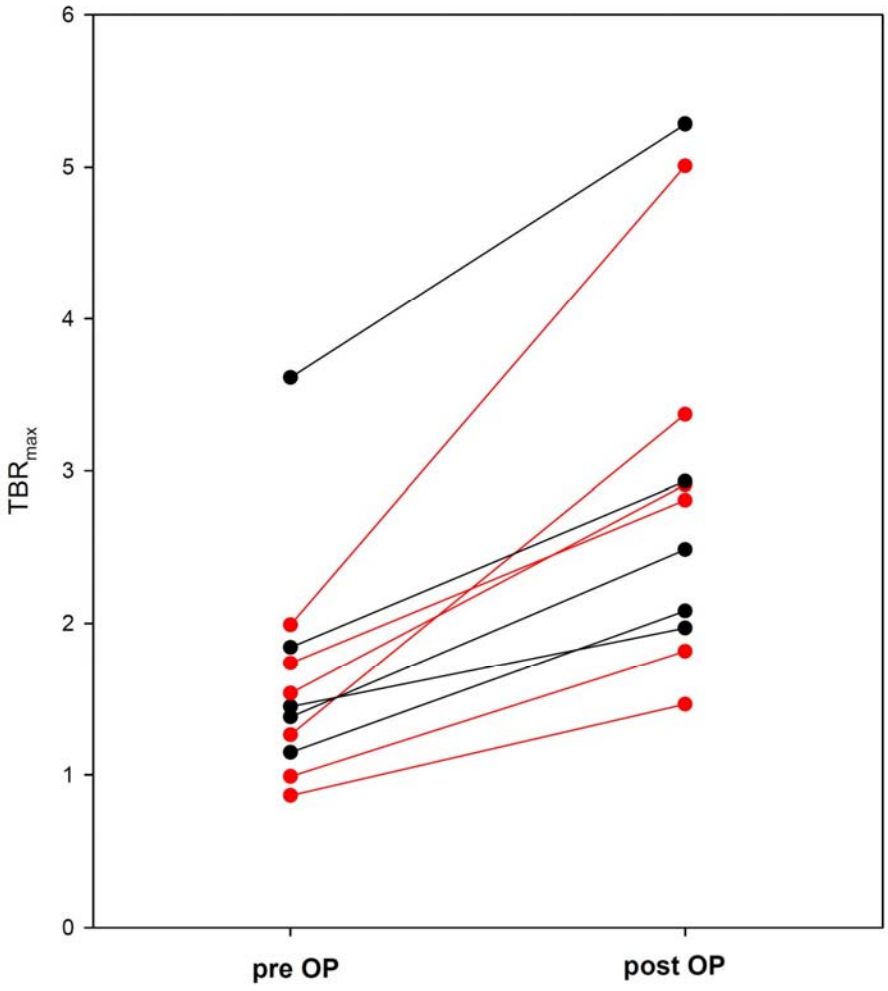

Changes of the TBR_{max} of ^{18}F-FET uptake in patients with a flare phenomenon after surgery i.e. either in the area of tumor tissue with increased ^{18}F-FET uptake in the preoperative scan (n=5, black symbols) or in an area distant to that location (n = 6, red symbols).

Figure 4:

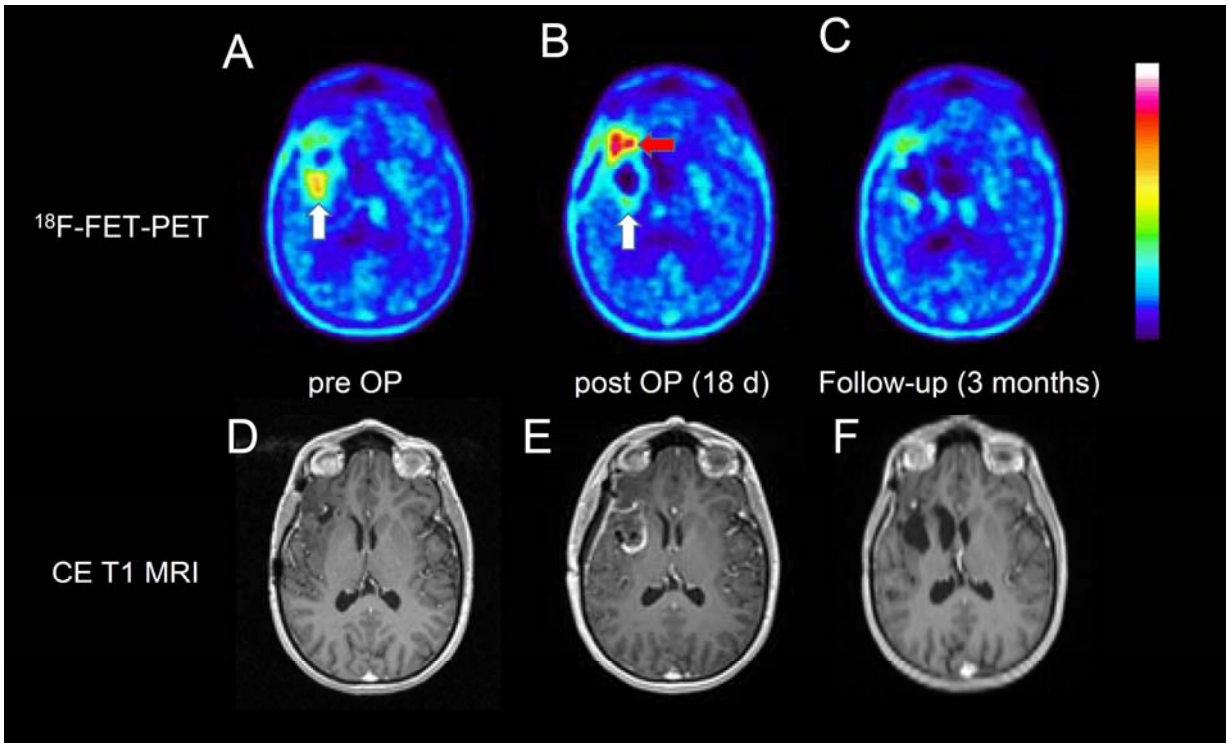

Axial images of a patient with fronto-temporal oligodendroglioma WHO grade III in the right hemisphere (Pat. No 33): Pre-, postoperative, and follow-up ^{18}F-FET PET (A - C), and contrast-enhanced T1-weighted MRI (D - F). PET after surgery (B) shows total resection of the ^{18}F-FET positive area (white arrow) in the preoperative scan (A), but a flare phenomenon is noted in the frontal area to the resection cavity (red arrow). A follow-up PET scan after chemotherapy shows a reduction of tracer uptake in that area (C).

SUPPLEMENTAL MATERIAL

Aquisition of ^{18}F-FET PET data

^{18}F-FET was produced via aminopolyether-activated nucleophilic ^{18}F-fluorination and applied as described previously (*1*). Dynamic PET data were acquired in list mode for 40 min after intravenous injection of approx. 2.5 MBq of ^{18}F-FET/kg of body weight. Seventy-nine scans were obtained using a stand-alone PET scanner (ECAT EXACT HR+, Siemens Healthcare, Erlangen, Germany) in 3D mode (32 rings, axial field of view, 15.5 cm). The reconstructed dynamic dataset consisted of 16 time-frames (5 x 1 min; 5 x 3 min; 6 x 5 min). A transmission scan (duration, 10 min) using three rotating line sources (^{68}Ge/^{68}Ga) was used for attenuation correction. Before iterative reconstruction based on ordered-subset expectation maximization (OSEM, 16 subsets, 6 iterations), data were corrected for dead time, random and scattered coincidences. Twenty-two scans were done on a high-resolution 3T hybrid PET/MR scanner (BrainPET, Siemens Healthcare, 72 rings, axial field of view, 19.2 cm). Image data were corrected for random and scatter coincidences, as well as dead time before OP-OSEM reconstruction provided by the manufacturer (2 subsets, 32 iterations). The reconstructed dynamic data set consisted of 16 time-frames (5 x 1 min; 5 x 3 min; 6 x 5 min). Since the hybrid PET/MR scanner does not provide a transmission source, attenuation correction was performed with a template-based approach using MRI (*2*). All dynamic ^{18}F-FET PET datasets were also corrected for motion before further processing. Based on the reconstruction parameters and post-processing steps used in the present work, the quantitative ^{18}F-FET PET parameters of the different scanner types are comparable (*3*).

PET data analysis

The time-activity curves (TAC) of ^{18}F-FET uptake in areas with flare phenomenon and in the corresponding areas before surgery were generated by the application of a spherical volume-of-interest (VOI) with a volume of 2 mL centered on maximal tumour uptake to the entire dynamic dataset as described previously (*4*). The time-to-peak (TTP; time in minutes from the beginning of the dynamic acquisition up to the maximum SUV of the lesion) and the slope of the TAC in the late phase of FET uptake was assessed by fitting a linear regression line to the late phase of the curve (11–40 min post-injection). The slope was expressed as the change of the SUV per hour. This allows for a more objective evaluation of kinetic data compared to an assignment of TACs to earlier reported patterns of ^{18}F-FET uptake during dynamic acquisition.

Supplemental Figure 1:

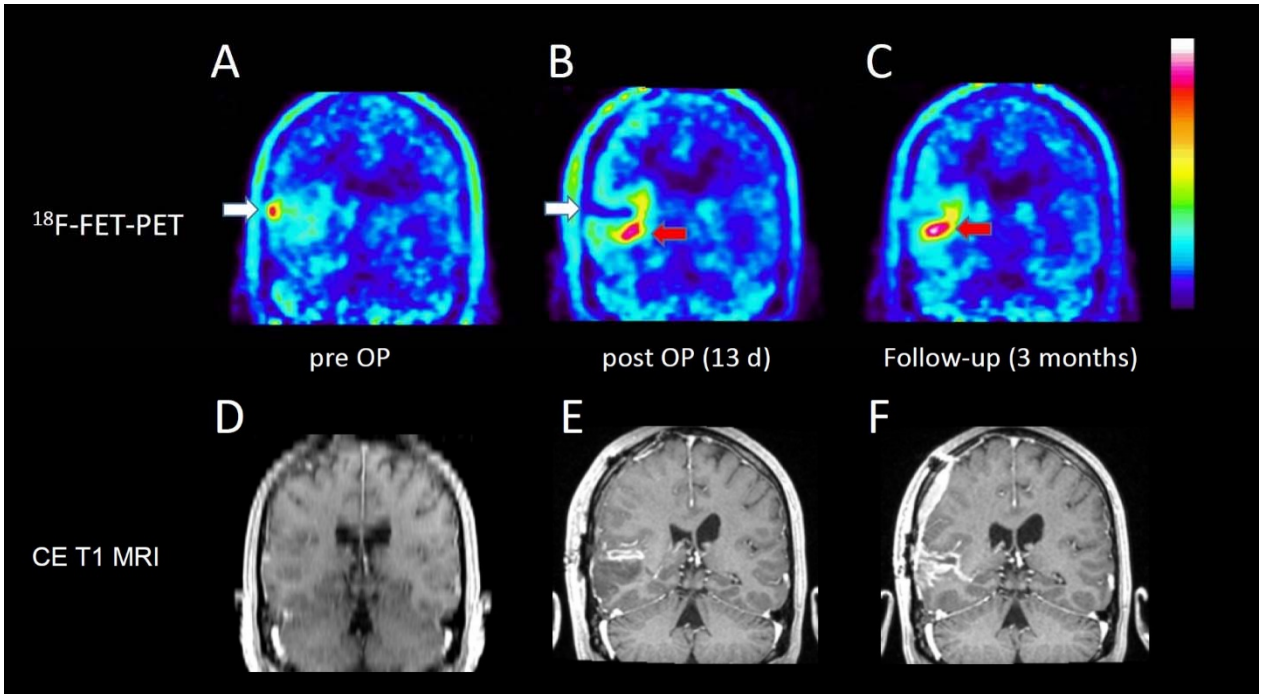

Coronal brain slices of a patient with temporal glioblastoma WHO grade IV in the right hemisphere (Pat. No 17): Pre-, postoperative, and follow-up ^{18}F-FET PET (A - C), and corresponding contrast-enhanced T1-weighted MRI (D - F). ^{18}F-FET PET after surgery (B) shows resection of the ^{18}F-FET positive area (white arrow) in the preoperative scan (A), but a flare phenomenon is noted medial to the resection cavity (red arrow). The follow-up PET after chemotherapy shows a progressive tumor in that area.

1. Hamacher K, Coenen HH. Efficient routine production of the 18F-labelled amino acid O-2-18F fluoroethyl-L-tyrosine. *Applied radiation and isotopes.* 2002;57:853-856.

2. Kops ER, Herzog H, Shah NJ. Comparison template-based with CT-based attenuation correction for hybrid MR/PET scanners. *EJNMMI Phys.* 2014;1:A47.

3. Lohmann P, Herzog H, Rota Kops E, et al. Dual-time-point O-(2-[(18)F]fluoroethyl)-L-tyrosine PET for grading of cerebral gliomas. *Eur Radiol.* 2015;25:3017-3024.

4. Galldiks N, Stoffels G, Filss C, et al. The use of dynamic O-(2-18F-fluoroethyl)-l-tyrosine PET in the diagnosis of patients with progressive and recurrent glioma. *Neuro Oncol.* 2015;17:1293-1300.